Using a laser aureole to study aerosols

Brandon J.N. Long, D. A. Hook, Garret E. Pangle, Hans D. Hallen, C. Russell Philbrick
Physics Department, NC State University, Raleigh NC, 27695-8202

ABSTRACT

Aerosol optical scattering experiments are often large, expensive, and provide poor control of dust uniformity and size distribution. The size distribution of such suspended atmospheric aerosols varies rapidly in time, since larger particles settle quickly. Even in large chambers, 10 micron particles settle in tens of seconds. We describe lab-scale experiments with stable particle distributions. A viscous colloidal solution can stabilize the particles for sufficient time to measure optical scattering properties. Colloids with different concentrations or size distributions enable nearly time independent studies of prepared distributions. We perform laser aureole scattering from a colloid containing a few percent by volume of Arizona Road Dust (ARD) in mineral oil and glycerin, and 1-micron polystyrene spheres in water. We discuss aureole analysis, the differences expected in scattering properties due to the index of refraction of the mineral oil medium versus air, and the impact of non-spherical shape on the scattering. This research demonstrates that particles suspended in a viscous medium can be used to simulate aerosol optical scattering in air, while enabling signal averaging, offering reproducibility, and easing problems resulting from parameter variations in studies of dust properties.

Keywords: laser aureole, aerosol scattering, Arizona Road Dust (ARD), laser scatter from colloid, optical properties of aerosols

1. INTRODUCTION

Aerosol optical scattering is important in many meteorological and atmospheric conditions. While optical signatures of many chemical and liquid aerosols are well characterized, mineral dust continues to be a problem because of its non-spherical shape [1], its complicated chemical makeup, and its widely varying size distribution. Optical properties of mineral dust are very important in understanding the planet's heat budget [1, 2] and atmospheric optical propagation measurements [3, 4, 5].

Experiments that directly measure aerosol dust scattering by using fans to continually mix the volume suffer from poor reproducibility and short measurement times. In air, particles larger than ~10 microns are difficult to stably suspend, and much material falls out of the suspension within tens of seconds, often before a distribution fully uniform in the volume is achieved. This method of suspending particles often causes changes in the actual size distribution and in the amount of material suspended. For example, smaller particles may be liberated from the surface of larger ones while passing through the injection nozzle by collisions with other particles or the nozzle itself.

The scattering aureole is advantageous for measuring bulk scattering, as it is independent of the particle eccentricity for values of eccentricity typically found in ARD [7]. Thus, the distribution of eccentricities need not be modeled, and Mie calculations are sufficient. The solar aureole was first measured in the 1960s to extract information about atmospheric particle size distributions [3, 4, 5]. Successful measurements using the aureole require care. A large chamber can be used to measure particle forward lobe scattering from a laser source with bistatic methods. Aureole measurements obtained by imaging a target board require a more careful analysis. If a chamber path is a significant fraction of the total path length (i.e., 1/3 the total path), then light rays, which are scattered at the same angle from the beginning to the end of the path through the chamber will end up at different points on a detector's surface.

Steps have been made to develop techniques that can directly measure scattering phase functions of aerosols in a lab environment [6], but the best method of dispensing the sample is still an issue. It is difficult to establish a uniform dispersal of coarse mode aerosols in air, due to their relatively high terminal velocities.

By suspending the dust in a more viscous medium, we significantly lower their terminal velocities. Agitating the colloidal suspension results in a long-term stable state; thereby permitting more accurate measurements and better

Laser Radar Technology and Applications XVIII, edited by Monte D. Turner, Gary W. Kamerman,
Proc. of SPIE Vol. 8731, 87310O · © 2013 SPIE · CCC code: 0277-786X/13/$18 · doi: 10.1117/12.2017707

reproducibility. If we limit measurements to the aureole, scattering at angles less than ~20 degrees, we can ignore the aspheric shape of our particles [7].

2. METHODS

2.1 Sample preparation

We selected two samples to use while proving this technique: ultrafine Arizona Road Dust (ARD), which is a standard commercially available dust, and one micron diameter polystyrene spheres, which provide a known size and shape. We selected a medium for the samples from mineral oil, glycerin, and water. For ARD, we immerse a container of a dust-oil mixture in a warm water bath. Ultrasonic agitation gives the dust particles enough energy to mix the particles through the entire solution. The process is relatively slow, and most samples had to be allowed to mix overnight. Glycerin mixtures are somewhat easier, as the ARD acts slightly hydrophilic, and glycerin is a polar molecule, so the dust suspends easily with short duration manual mixing. It stays suspended longer than in the mineral oil. The sonication does not impart enough momentum to overcome a relatively high settling speed of large particles in ARD with water as the medium. The water also appears to wash the particles, leach metal ions from the dust particles, and otherwise change the particles, so we do not use it for ARD. The calibration samples, which are polystyrene spheres of 1-micron in diameter, are shipped in water. We wash them and re-suspend them at the proper concentration easily via manual mixing.

A good measure of settling time of larger particles in the suspension is the vertical extent of the measurement volume divided by the terminal velocity. This is easily calculated by the Stokes flow around a sphere with some buoyancy,

$$v_t = \frac{gd}{18\mu}(\rho_s - \rho), \tag{1}$$

where g is gravitational acceleration, d is the diameter, ρ is the density of the fluid, $\rho_s$is the density of the sphere, and μ is the viscosity of the medium [8]. Using the terminal velocity, we can calculate the time needed to fall one millimeter, which is the size of the laser beam in the solution, see Table 1. We calculate the settling time for a 14 micron diameter silica sphere as a representative large ARD particle; for a small particle, we use a 2-micron silica sphere. When the depth of the solution is much larger than the laser beam size, we can replace the one millimeter with the distance from the laser beam to the top of the fluid volume. The times in Table 1 can then be multiplied by (the distance to the top)/(1 mm).

Table 1: Settling times calculated for one mm fall of our samples through several media. Air was not used in this experiment, but is provided as reference.

Media	Settle time for polystyrene (s)	Settle time for coarse-mode (14-µm) ARD (s)	Settle time for small course-mode (2-µm) ARD (s)
Glycerin	$1.69 * 10^6$	$8.65 * 10^3$	$4.24 * 10^5$
Water	$1.18 * 10^3$	6.01	$2.95 * 10^2$
Mineral Oil	$1.31 * 10^4$	$6.67 * 10^1$	$3.27 * 10^3$
Air	13.0	$6.62 * 10^{-2}$	3.24

Since our measurements are made in a viscous medium, our settling times are much longer than in air. Conventional chamber measurements must take into account a continuously changing size distribution, as the re-lofting of particles or upwelling of air are not particularly effective at extending the measurement period. Figure 1 shows APS data from a chamber measurement, which demonstrates the changes in the size distribution. With our long settle times, we can take data for a long period of time to obtain good statistics, and be confident that the samples' distributions did not drastically change, as they do in chamber measurements. We can take the distribution from anywhere, for example, by lofting the dust and waiting a certain amount of time before collecting a sample. Thus, we are able to replicate data taken in air with more accuracy.

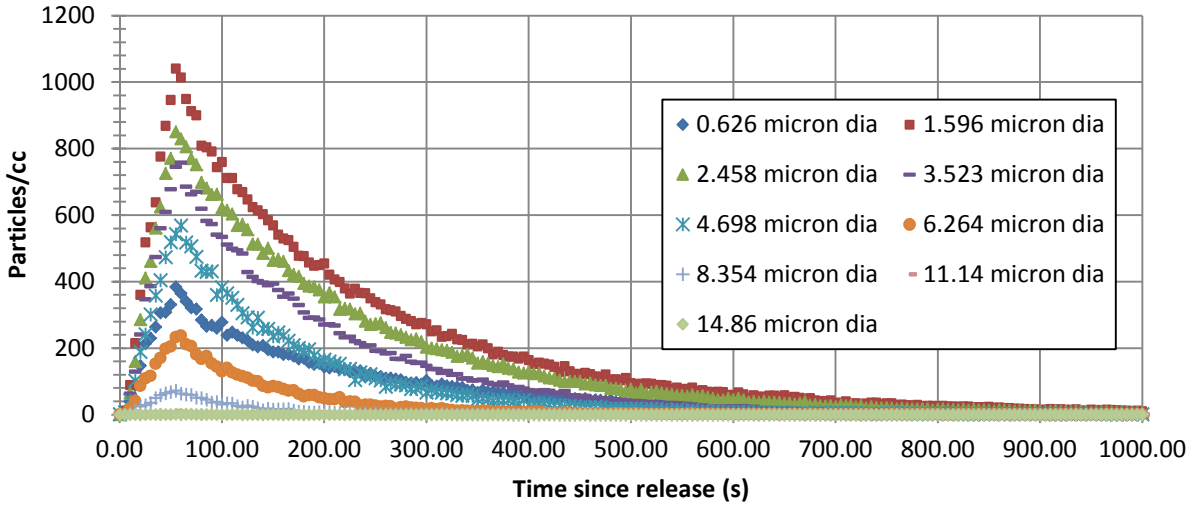

(a)

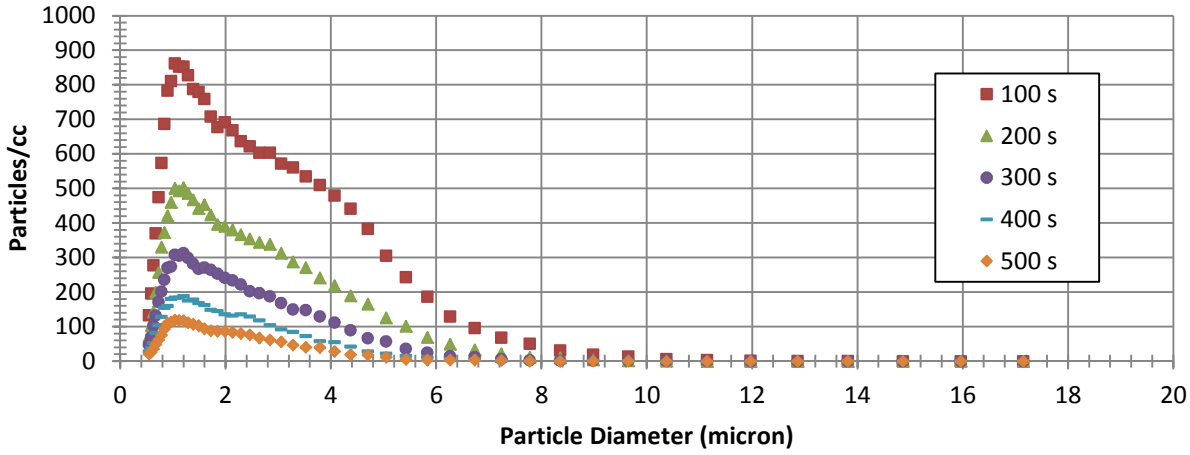

(b)

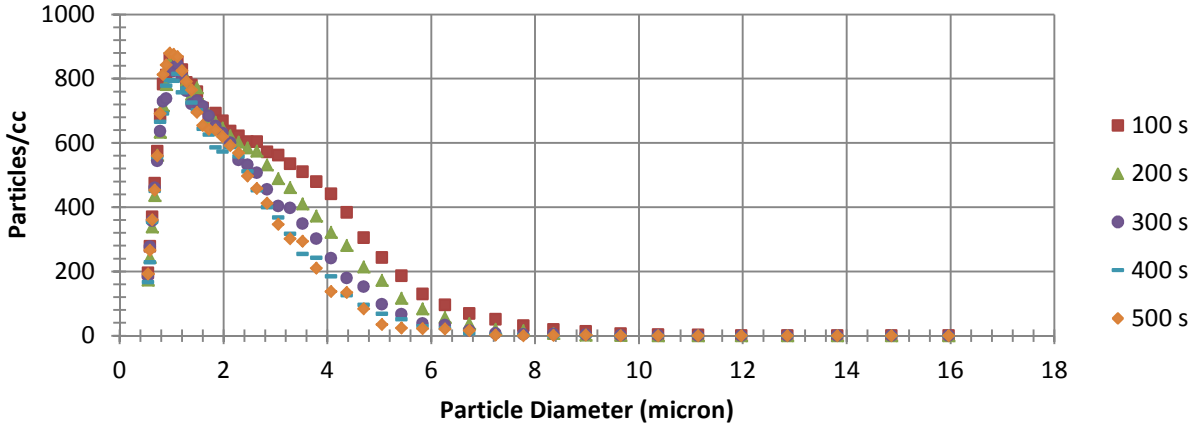

(c)

Figure 1. Chamber measurements of size distribution. (a) shows how several size cuts change after release, (b) shows five representative size distributions at certain time cuts, and (c) shows the same size distributions scaled so that all have the same peak height at 1.3 microns, to better show the changing structure.

2.2 Data collection

Our experimental apparatus is shown in Figure 2. Two detectors are mounted around a polarizing beam splitting cube, which is attached to a long arm driven by a geared down stepper motor. A laser of a known wavelength (473 nm) passes through a cuvette centered above the axis of rotation of the arm. The detectors collect scattering data as they swing through a large range of angles. The cuvettes were rotated slightly to minimize the Fresnel reflections' effects on the data.

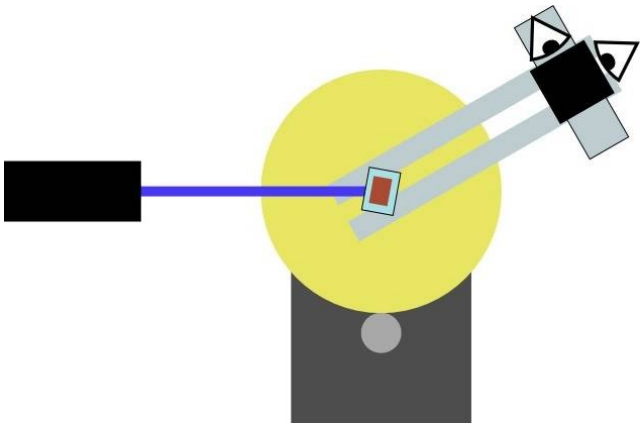

Figure 2. The scattering apparatus uses a laser that passes through the cuvette and polarization-dependent scattering is measured by the detectors behind the polarizing cube.

2.3 Mie Calculations

Within the aureole, Mie calculations are an accurate way to predict the scattering data profile. We use the code provided by Bohren and Huffman's book [9], which we translated to C and modified the conditions to select the number of terms in the series to calculate the scattering of small particles. We use the manufacturer's supplied normalized size distribution for the ARD, and a narrow distribution centered at 1-μm for the polystyrene spheres from Polysciences, Inc. These are scaled by our concentration to determine an equivalent size distribution of spheres. The distributions are shown in Figure 3. We assume that the index of refraction of ARD does not differ from silica. Our other materials are much better documented, and are summarized in Table 2. The only free parameter in the modeling (besides the estimate for ARD index, which we do not vary) is a scaling factor for the detector's sensitivity.

Table 2: List of indices of refraction used in calculations.

Material	Index of Refraction	Reference
Glycerin	1.473	[10], [11]
Polystyrene	1.613	[12]
Mineral oil	1.47	[11]
ARD (as Silica, see text)	1.458	[13]
KBr	1.574	[14]

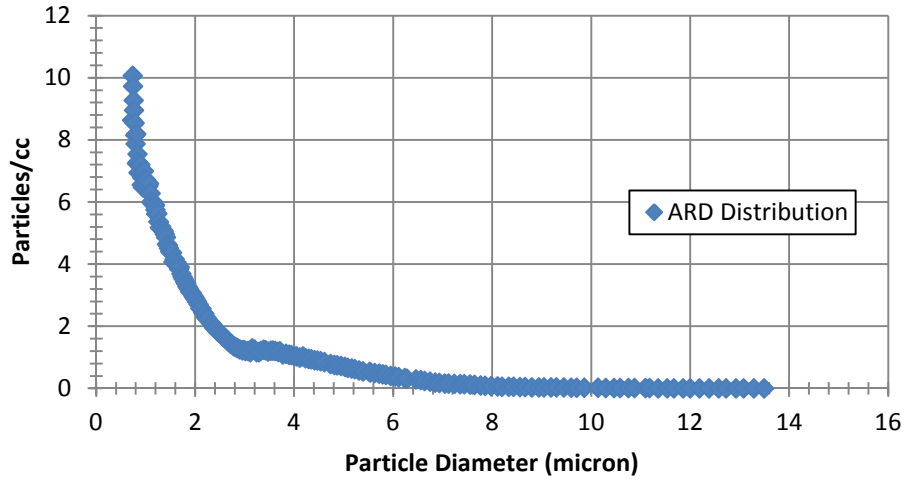

(a)

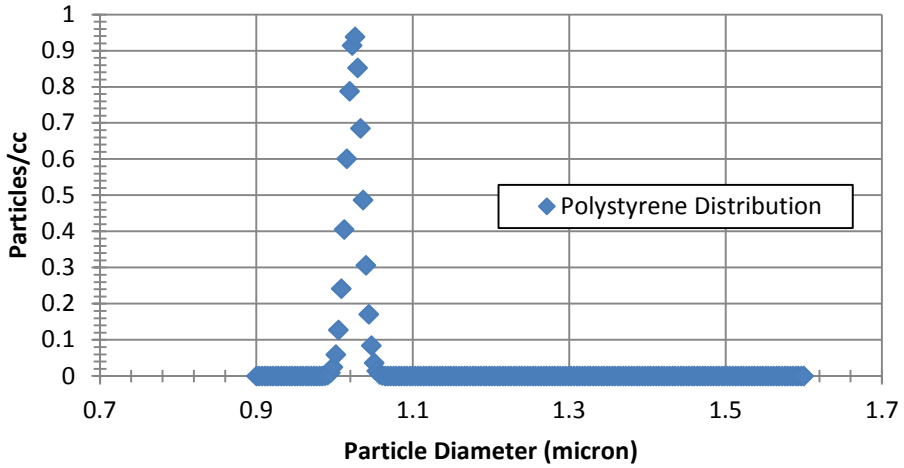

(b)

Figure 3. The size distribution used for (a) ARD, and (b) polystyrene spheres in our Mie calculations. The size distributions are known and the indicies of refraction are listed in Table 2. The only free parameter is the detector sensitivity.

2.4 Pellet Measurements

In addition to colloids, we use KBr pellets to measure scattering. The solid pellet has several advantages: no particles fall out, a different index of refraction from the oils, and complete control over size distribution and mixing. However, we had to use great care in sample preparation to keep background scatter from micro-fissures and KBr's hygroscopic qualities from overwhelming ARD's scattered signal. Since our polystyrene spheres were packed in water, we were unable to use them in these pellets to confirm our data, as they would introduce too much moisture into the KBr, causing fogging.

3. DATA

3.1 KBr pellets

The KBr pellets were prepared with 0.1% bV ARD. Since the pellets are on average 1 mm in path length, compared to the 1 cm cuvette path length, this is still within our range of single-scatter phenomena. Scattering measurements with incident laser light polarized perpendicular to the plane of scattering are plotted with Mie scattering calculations and fit in Figure 4. The silica sphere calculations and the measured scatter do not agree. This is likely due to an erroneous index of refraction. When we let n_ARD vary, we are able to fit both KBr and colloid scatter. In this fit, we found n_ARD=1.56. . The calculation assumes that there is no loss in the pellet and only Fresnel reflection losses at the surfaces. Defects in the pellet may cause additional loss, which reduces the measured signal at these larger angles/path lengths.

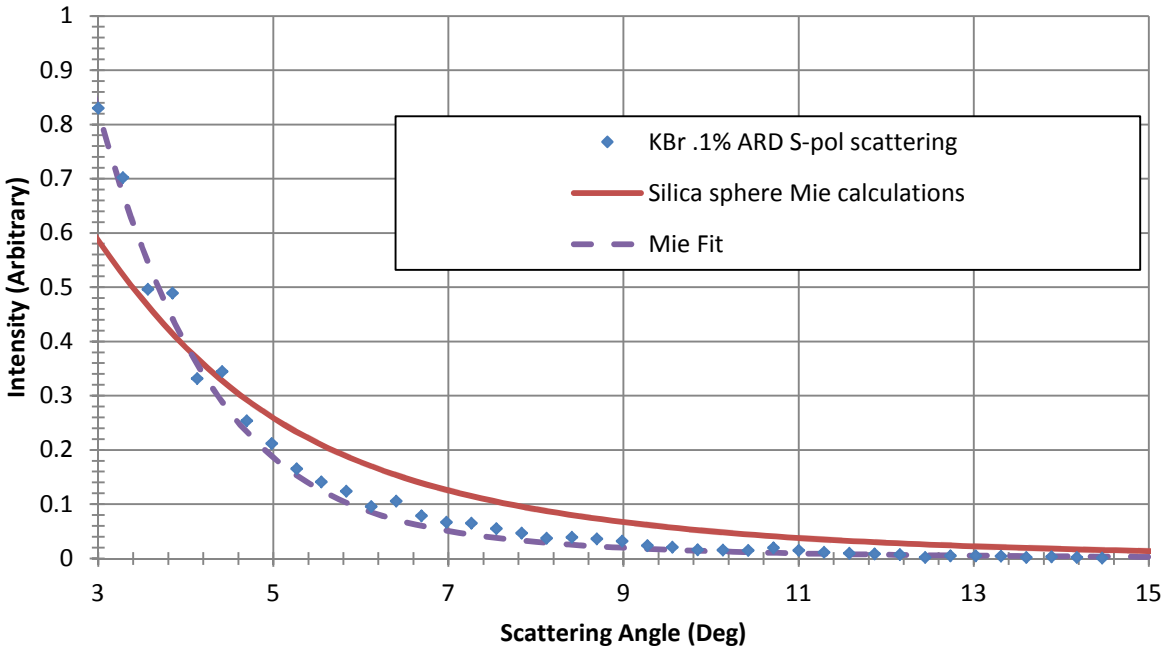

Figure 4. Optical scattering data for the S-polarization is compared with Mie calculations and fit.

3.2 Polystyrene Spheres

The 1-micron diameter polystyrene spheres are suspended in water to measure their scattering. Figure 6 shows scattering measurements made of a colloid with 0.001333% by volume (bV) of polystyrene spheres using the Mie calculations with refractive index from the manufacturer's data. The two sets show good agreement, which indicates the system is well calibrated.

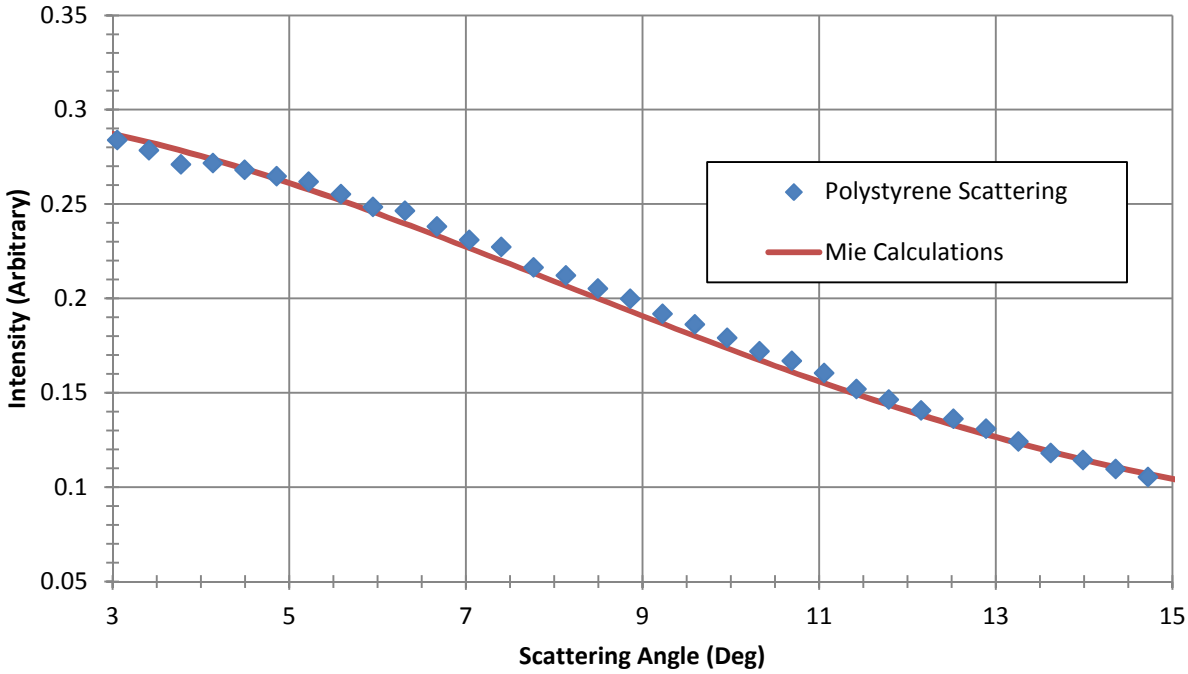

Figure 5. Scattering data and forward calculations for a 0.001333% bV polystyrene sphere/water colloid.

3.3 Ultrafine Arizona Road Dust (ARD)

We used two colloids to study the ARD scattering properties; a mineral oil colloid 0.00105 % bV ARD, and a glycerin colloid 0.001285% bV ARD. The scattering measurements are shown in Figure 7, where both the scattering of light initially polarized perpendicular to the scattering plane that remains in that plane, and the depolarized scatter are presented. Both sets of data agreed very closely, as shown in Figure 8, which indicates that the system was working as intended. Specifically, it indicates both samples are structured the same, despite the different ways of getting the dust into a colloid. In particular, these solvents do not tear apart the complex structure of the particles, as water does. Both data sets are compared with silica sphere forward calculations in Figure 9. The data shows poor agreement here, which probably indicates that the index of refraction of the ARD cannot be approximated by that of silica. The fit is calculated by varying n_{ARD}. Here, we found n_{ARD}=1.56 fits best. Figure 10 shows KBr scatter compared to both glycerin and mineral oil scatter. The differences are likely due to the difference in index of refraction of the medium. The size parameter in Mie calculations, $ka = 2\pi a/\lambda$ for λ the wavelength of light in the medium and a the sphere radius, depends linearly on the medium's index of refraction through the inverse wavelength. Thus, a higher index for the medium KBr compared to mineral oil and glycerin (with nearly the same index) should result in a narrower scattering lobe for the KBr sample. This is qualitatively observed in the plots.

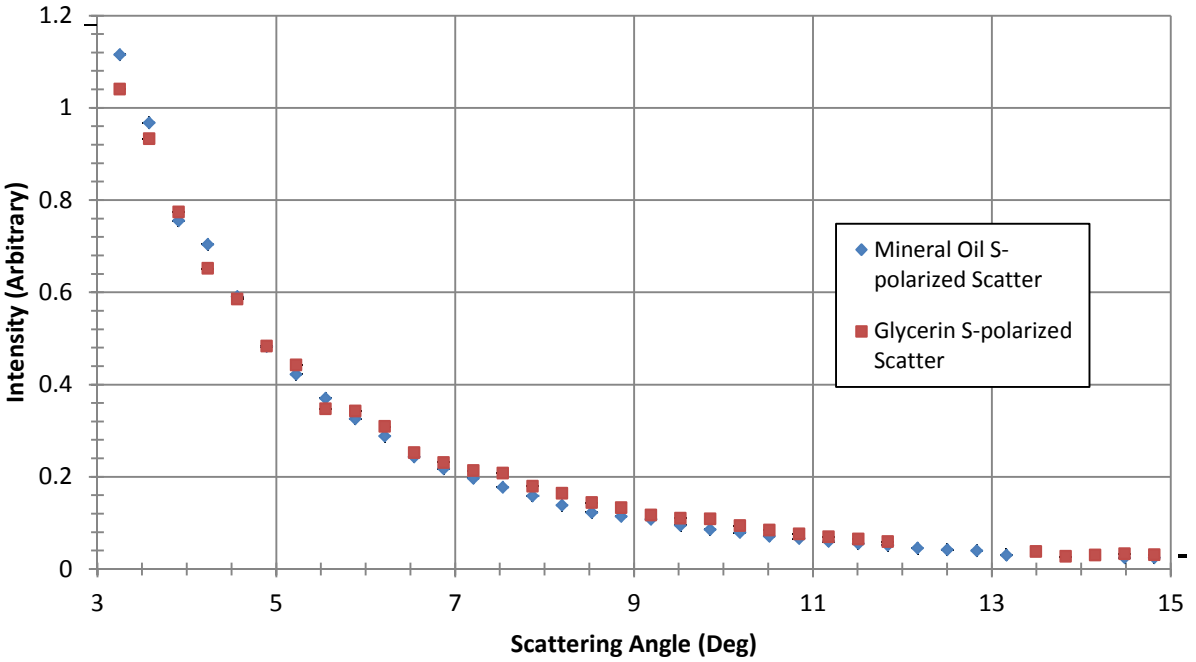

(a)

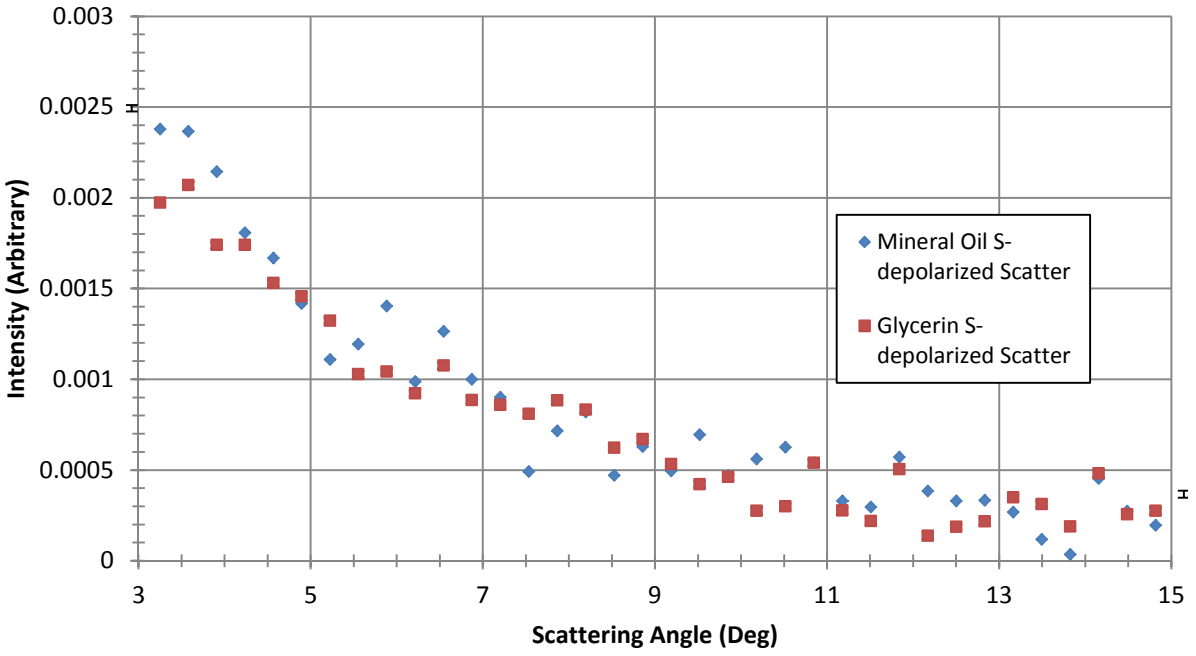

(b)

Figure 6. Scattering data from ARD in a 0.00105% bV colloid with mineral oil and 0.00129% bV glycerin shows (a) S-polarized scatter and (b) depolarized scatter.

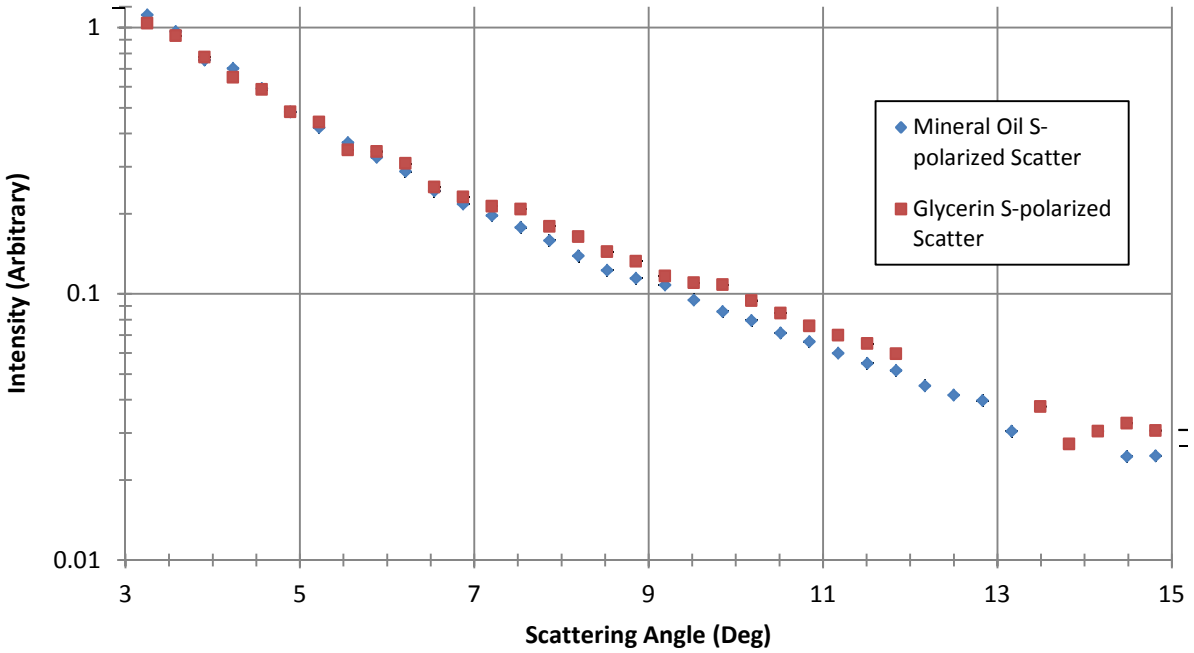

(a)

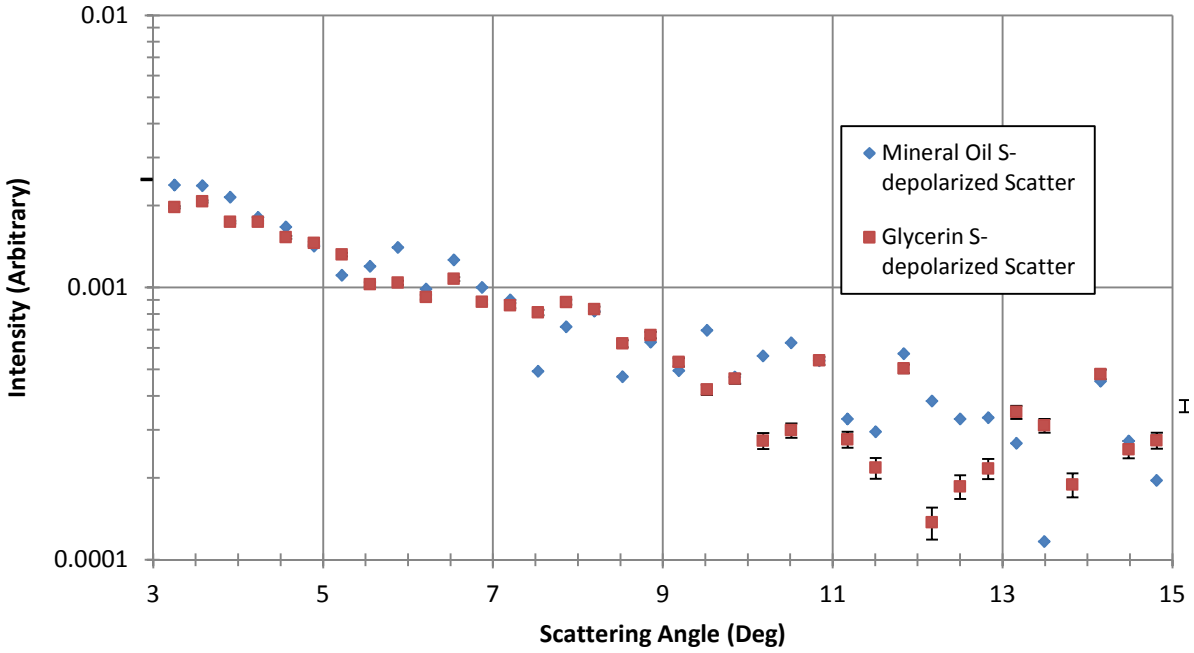

(b)

Figure 7. Semi-log plots of the same data as in Figure 6.

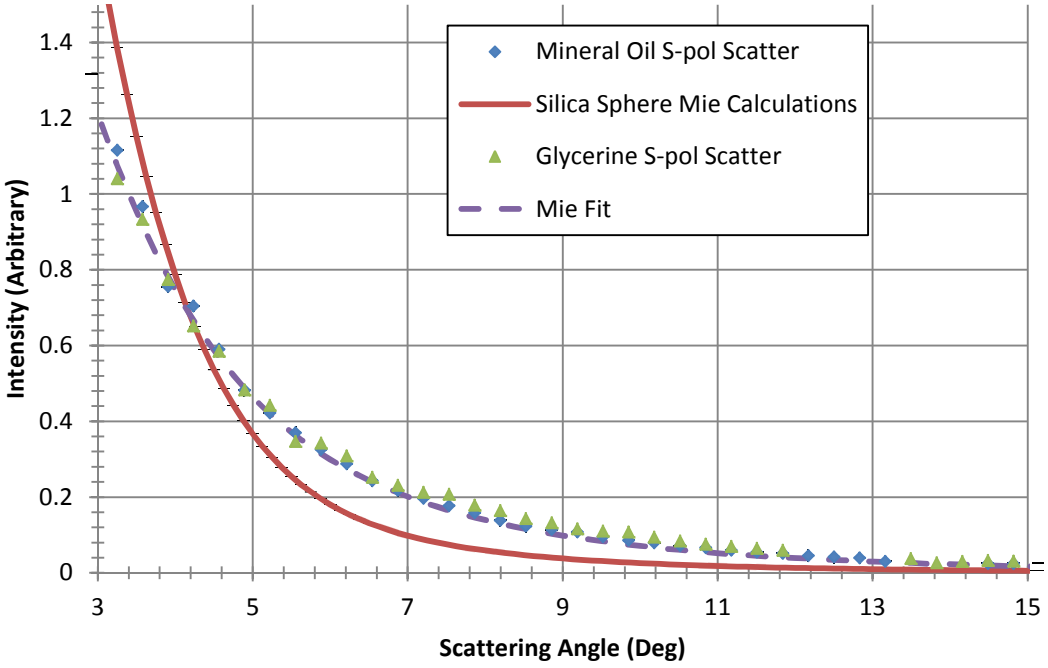

Figure 8. The ARD colloids plotted with equivalent size silica sphere scattering calculations and fit.

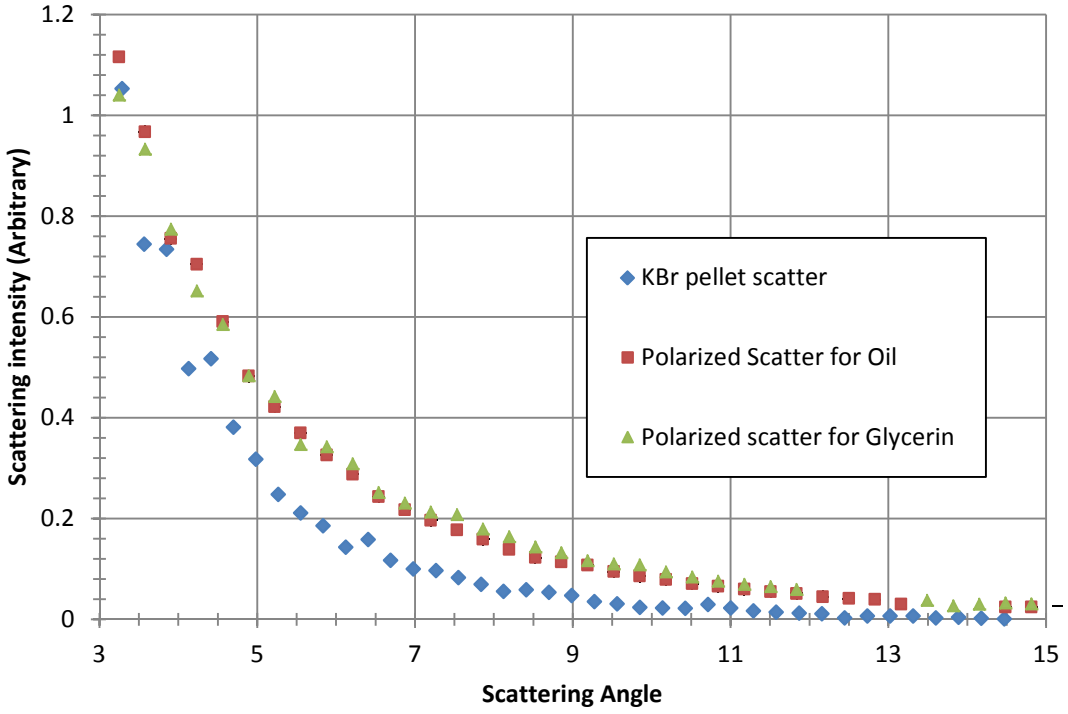

Figure 9. The scattering data for glycerin and mineral oil colloids, and KBr pellet plotted together. Note that the KBr scatter differs from the scatter of the colloids.

4. ANALYSIS

4.1 Medium to air corrections

The propagation at non-normal incidence through the flat interface between the cuvette and air means the scattering angle is not directly measured, but must be calculated based on the physical geometry. The refracted beams appear to come from an illusory center, but that correction is negligible (i.e., $\varphi_{meas} \approx \varphi_0 - \theta$). A geometric calculation using Snell's law determines that

$$\theta_s = \sin^{-1}\left(\frac{\sin(\varphi_{meas} + \theta)}{n}\right) - \theta_t, \tag{2}$$

where the angles are defined in Figure 11, and φ_{meas} is the measured angle.

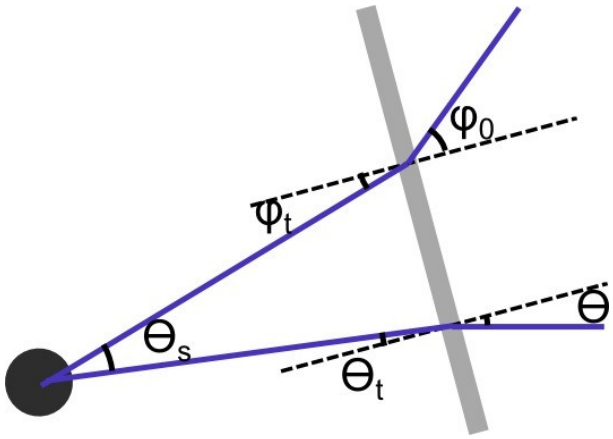

Figure 10. The angles defined for the scattering correction equation above.

The measured intensities are corrected for the transmission through the interface using the Fresnel formulae. The scattered rays pass through a longer path in the scattering material, thus extinct more, but this is negligible for a standard cuvette. A KBr pellet, containing more scattering material per unit volume, is affected by this extinction.

4.2 Comparison of measurements and simulations

The polystyrene sphere data, shown in Figure 6, provide confidence in our measurements. The predictions differ somewhat near the edge of the range, but this may be due to internal reflections of the cuvette. The reasonably close agreement demonstrates that valid measurements of aerosols can be made using colloids.

The results in Figure 8 show ARD scatter does not agree well with Mie calculations for silica spheres. Good results from Mie calculations in modeling ARD have been shown in past experiments [15]. The shape of the ARD particles is approximately ellipsoidal with an a/b ratio less than ~1.5, thus Mie calculations are expected to work well in the aureole [7]. The most likely reason for failure is the assumption of silica-like particles. In other words, the failure could simply be that the wrong index of refraction is used, or that the particles are in a core and shell arrangement, which would alter the scattering properties. Letting the n_{ARD} vary allows us to fit both KBr and the colloid suspensions. In this case, we found n_{ARD} to be 1.56, which is quite different from silica. The fact that ARD is not only silica is verified by careful studies of dust [15, 16].

The two ARD data sets in different media reproduce each other very well, as shown in Fig. 7. This indicates the basic functionality of the method. When the indices of the media are the same, the results are. It also indicates that particles of dust can be placed into these fluids and not be altered in either geometry or chemistry by the fluid. We would not expect similar results in water, which removes minerals from the dust particles. The measurement technique is valid, despite the

unknown ARD index. Another presentation at this conference describes measurements of the index of refraction of particles [16].

Scattering by ARD in KBr differs from that when it is immersed in the glycerin and mineral oil. Since KBr has a different index of refraction, the size parameter in Mie scattering changes, and this changes the width of the aureole and location of the scattering resonances. We see evidence for these differences in the measurements. The silica sphere calculations failed to predict the scattering, as in the colloids. We fit n_{ARD}=1.56 using both data sets, which is further evidence for the correctness of the fit.

5. CONCLUSIONS

Using bulk samples in colloids instead of aerosols in air, we avoided many of the problems in these standard experiments. A quantitative verification of the measurement technique was made with polystyrene spheres, which are well described by Mie calculations. The optical properties of dust are reported using samples of ARD with two different ways of suspending the sample in solution. The colloids of non-spherical ARD particles matched each other closely for suspensions in mineral oil and glycerin, which gives further confidence in the measurement approach. Measurements in KBr agree well with Mie calculations using equivalent size silica spheres. However, the colloid results are not in good agreement with Mie calculations when the index of refraction for silica is used. The solution to this problem is to let the index of refraction of ARD vary. Here, it is shown that n_{ARD}=1.56. This shows the use of colloidal solutions to study aerosol optical scattering is a useful technique.

REFERENCES

[1] Dubovik, O.,,Holben, B. N., Lapyonok, T., Sinyuk, A., Mishchenko, M. I., Yang, P., Slutsker, I., "Non-spherical aerosol retrieval method employing light scattering by spheroids," Geophys. Res. Lett. 29 (10), 54-1-54-4 (2002)

[2] Mallet, M., Tulet, P., Serca, D., Solmon, F., Dubovik, O., Pelon, J., Pont, V., Thouron, O., "Impact of dust aerosols on the radiative budget, surface heat fluxes, heating rate profiles and convective activity over West Africa during March 2006," Atmos. Chem. Phys. 9 (18), 7143-7160. (2009)

[3] Eiden, R., "Calculations and measurements of the spectral radiance of the solar aureole," Tellus XX, 380-399 (1968);

[4] Box, M., and A. Deepak, "Retrieval of aerosol size distributions by inversion of simulated aureole data in the presence of multiple scattering," Appl. Opt. 18, 1376-1382 (1979).

[5] Volz, F., "Measurements of the skylight scattering function," Applied Optics 26 (19), 4098-4105 (1987).

[6] Muñoz, O., Moreno, F., Guirado, D., Ramos, J., L., López, A., Girela, F., Jerónimo, J., M., Costillo, L., P., Bustamante, I., "Experimental determination of scattering matrices of dust particles at visible wavelengths: The IAA light scattering apparatus," J. Quant. Spectros. Radiat. Transfer 111 (1), 187 – 196 (2010)

[7] Hallen, H. D., Hook, D. A., Pangle, G. E., Philbrick, C. R., "Multistatic lidar measurements of non-spherical particles," SPIE Proc. 8731-25, 2013 (this proceedings).

[8] Nguyen, A.V., Stechemesser, H., Zobel, G., Schulze, H.J., "An improved formula for terminal velocity of rigid spheres," Int. J. Min. Process. 50 (1–2), 53-61 (1997)

[9] Bohren, C. F., Huffman, D. R., [Absorption and scattering of light by small particles], Wiley-VCH (2007)

[10] Weast, R.C., [CRC Handbook of Chemistry and Physics. Ed. 62 Edition], CRC Press, Boca Raton, Fl., E155. (1981)

[11] Poulter, T. C., Ritchey, C., Benz, C. A, "The effect of pressure on the index of refraction of paraffin oil and glycerine," Phys. Rev. 41 (3), 366 – 367 (1932)

[12] Kasarova, S.N., et al. "Analysis of the dispersion of optical plastic materials," Opt. Mater. 29, 1481-1490 (2007)

[13] Hecht, E., [Optics, Fourth Edition], Pearson Higher Education (2003)

[14] Bass, M., DeCusatis, C., Enoch, J., Lakshminarayanan, V., Li, G., MacDonald, C., Mahajan, V., Van Stryland, E., [Handbook of Optics, 3rd edition, Volume 4], McGraw-Hill (2009)

[15] Curtis, D., B., Meland, B., Aycibin, M., Arnold, N., P., Grassian, V., H., Young, M., A., Kleiber, P., D., "A laboratory investigation of light scattering from representative components of mineral dust aerosol at a wavelength of 550 nm," J. Geophys. Res., 113, D08201, (2008)

[16] Hook, D. A., Pangle, G. E., Hallen, H. D., Philbrick, C. R., "Understanding lidar returns from complex dust mixtures," SPIE Proc. 8731-22 (2013) (this proceedings).